Journal of Power Sources 220 (2012) 391–398

Contents lists available at SciVerse ScienceDirect

Journal of Power Sources

journal homepage: www.elsevier.com/locate/jpowsour

CoO nanocrystals as a highly active catalyst for the generation of hydrogen from hydrolysis of sodium borohydride

Aolin Lu, Yuanzhi Chen*, Jiarui Jin, Guang-Hui Yue, Dong-Liang Peng**

Department of Materials Science and Engineering, College of Materials, Xiamen University, 422 Siming South Road, Xiamen 361005, People's Republic of China

HIGHLIGHTS

- A new catalyst for the generation of H_2 from hydrolysis of $NaBH_4$ has been found.
- Octahedral and near-spherical CoO nanocrystals exhibit excellent catalytic property.
- A maximum H_2 generation rate of 8333 ml min^{-1} g^{-1} has been obtained at 303 K.
- Exposed crystal facets make differences to the catalytic behavior.
- CoO nanocrystals can be a promising candidate for substituting noble metal catalyst.

GRAPHICAL ABSTRACT

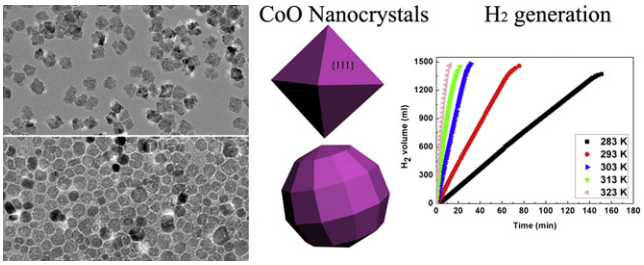

ARTICLE INFO

Article history:
Received 10 June 2012
Received in revised form
2 August 2012
Accepted 6 August 2012
Available online 12 August 2012

Keywords:
Cobalt(II) oxide
Hydrogen generation
Sodium borohydride
Hydrolysis
Catalyst

ABSTRACT

We report the excellent catalytic performance of CoO nanocrystals on the catalytic hydrolysis of alkaline $NaBH_4$ solutions. CoO nanocrystals with octahedral and near-spherical shapes are synthesized using a facile chemical solution method that employed cobalt acetate tetrahydrate as metal precursor in the presence of oleylamine. The octahedral CoO nanocrystals typically have a size of 40–50 nm, while the near-spherical nanocrystals have a size varying from 8 to 13 nm. Both of them have a face centered cubic (fcc) crystalline phase. Catalytic tests show that the as-synthesized CoO nanocrystals exhibit very high activities for the H_2 generation from the hydrolysis of alkaline $NaBH_4$ solutions. The maximum hydrogen generation rate of the as-synthesized CoO nanocrystals exceeds most reported values of transition metal or noble metal contained catalysts performed in alkaline $NaBH_4$ solutions. The influences of shape on the catalytic behaviors of as-synthesized CoO nanocrystals are also compared and analyzed. The results presented in this study indicate that CoO nanocrystals are a promising candidate to replace noble metal catalysts in the H_2 generation from the hydrolysis of borohydrides.

1. Introduction

Hydrogen is regarded as a clean and efficient fuel and an excellent substitute for fossil fuels. For fuel cell applications, hydrogen is recognized as environmentally desirable anodic fuel to generate electricity. However, many problems have to be resolved for safe and convenient usage of hydrogen energy. One of them is to seek for ideal hydrogen storage materials and effective method to control the storage and release of hydrogen. At present, chemical hydrides such as sodium borohydride are considered as a convenient hydrogen source with high densities of hydrogen available, and it is critical to explore suitable catalysts to control hydrogen release [1]. Hydrogen generation reaction upon $NaBH_4$ hydrolysis at

* Corresponding author. Tel.: +86 592 2188025; fax: +86 592 2183515.
** Corresponding author. Tel.: +86 592 2180155.
E-mail addresses: yuanzhi@xmu.edu.cn (Y. Chen), dlpeng@xmu.edu.cn (D.-L. Peng).

0378-7753/$ – see front matter © 2012 Elsevier B.V. All rights reserved.
http://dx.doi.org/10.1016/j.jpowsour.2012.08.010

ambient temperature in the presence of suitable catalysts is shown as follow [2]:

$$NaBH_4 + 2H_2O \xrightarrow{Catalyst} NaBO_2 + 4H_2$$

Catalysts that demonstrate high efficiency toward the reaction above usually contain noble metals such as Pt/C [3], Pd/C [4], PtRu/metal oxide [5], Ru/anion-exchange resin [6], Ag–Ni core–shell nanoparticles [7] etc. In addition, Au–Co [8] and Co–Pt core–shell nanoparticles [9] have also been reported to be very active in the catalytic hydrolysis of ammonia borane. However, owing to the high cost and limited availability of noble metals, it is essential to looking for low-cost catalysts for large-scale industrial production. Although many non-noble metals and metal oxides also demonstrate the ability to catalyze the hydrolysis of borohydrides, their catalytic activities are inferior to the noble metal catalysts. Cobalt-based catalysts are one kind of promising candidates to replace precious metal catalysts [10]. A couple of studies have been conducted on the catalytic performance of cobalt-based catalysts on the hydrolysis of borohydrides. For example, Co_3O_4, the stable phase of cobalt oxide was utilized as a catalyst for hydrolysis of borohydrides, however its induce time for the transformation to active Co–B phase was long [10–12]. Co–P–B amorphous powder which was produced by reducing $CoCl_2$ using $NaBH_4$ and NaH_2PO_2 was found with high activity and the ratio of B/P was influential [13]. Among these cobalt-based catalysts, amorphous Co–B and its related compounds displayed relatively high activity. In fact, many cobalt-based catalysts reported would convert to amorphous Co–B in catalytic process, but the catalytic behaviors were various [10–15]. It is worthy to be mentioned that hardly any attention has been paid to CoO materials on the catalytic performance for the H_2 generation from the hydrolysis of borohydrides.

CoO nanocrystals have received great attention due to their magnetic, catalytic, and electrochemical properties [16–19]. CoO also has been explored as a component of multi-oxide catalyst or a single catalyst for hydrodesulfurization [20] and CO oxidation [21]. For nanoscale CoO, studies often focus on its shape-control synthesis and properties mentioned above. For example, Nam synthesized CoO nano cubes and studied the electrochemical behaviors [16]. Wang et al. reported the synthesis of octahedral CoO nanocrystals with sizes of 200 nm or even larger and characterized the electrochemical performance [19]. Zhang et al. prepared CoO nanocrystals with various morphologies by turning surfactant concentration [22]. In contrast, reports are very rare on the catalytic properties of CoO material on the hydrolysis of chemical hydrides. Normally metallic Co is expected to be more reactive than its oxide counterpart as regard to the catalytic properties. Whether nanoscale CoO can perform well to promote the hydrolysis of chemical hydrides is an unsolved but interesting issue that deserves to be explored.

Previously we reported the excellent catalytic properties of Ag–Ni core–shell nanoparticles for the hydrogen generation from $NaBH_4$ hydrolysis [7]. In this study, we present important results on the catalytic properties of CoO nanocrystals for the same catalytic system. We first demonstrate a simple route for the synthesis of near-spherical and octahedral CoO nanocrystals. Then the catalytic behaviors under different reaction parameters were investigated. The results show that the as-prepared CoO nanocrystals exhibit unexpectedly very high activity toward $NaBH_4$ hydrolysis. In addition, the influences of crystal shape on the catalytic properties were investigated. Our results demonstrate that CoO nanocrystals can be an excellent candidate for substituting noble metal catalysts for the generation of H_2 from the dehydrogenation of borohydrides to satisfy the demands for green energies in multiple applications.

2. Experimental

2.1. Preparation of octahedral CoO nanocrystals

In a typical synthesis, 0.5 mmol of cobalt acetate tetrahydrate ($Co(OAc)_2 \cdot 4H_2O$) and 10 ml of oleylamine were placed into a reaction flask, and then the mixed solution was heated to 120 °C under vigorous stirring and kept at this temperature for 30 min to remove water. After the solution was cooled down to 90 °C, 1.5 mmol of trioctylphosphine (TOP) was injected into the solution, and the solution was further heated up to 240 °C and maintained at this temperature for 40 min before cooling down to room temperature. 10 ml of acetone was then added to the brown suspension and centrifugation was employed to separate the product. The obtained precipitate was then washed with hexane three times and dried in air.

2.2. Preparation of near-spherical CoO nanocrystals

In a typical synthesis, 0.5 mmol of $Co(OAc)_2 \cdot 4H_2O$ was dissolved into 10 ml of dibenzyl ether, resulting in a blue–purple solution. The solution was heated up to 130 °C under vigorous stirring and kept at this temperature for 30 min. After that, 1.5 ml of oleylamine was then injected into the solution, and the mixture was further heated up to 230 °C and kept at this temperature for 1 h. Then the solution temperature was fast increased to 260 °C, and maintained at this temperature for half an hour before cooling down to room temperature. The washing and collecting steps were similar to those for octahedral nanocrystals described above.

2.3. Characterization

Powder X-ray diffraction (XRD) patterns were recorded on a Panalytical X'pert PRO X-ray diffractometer using Cu K_α radiation. Scanning electron microscopy (SEM) was performed on a LEO-1530 scanning electron microscope. Transmission electron microscopy (TEM) data was collected on a JEM-2100 transmission electron microscope operating at 200 kV. X-ray photoelectron spectroscopy (XPS) analyses were performed using a PHI Quantum 2000 scanning ESCA Microprobe spectrometer using an Al K_α photon source.

2.4. Catalytic test

In a typical experiment, a flask containing 10 mg of as-prepared CoO catalysts was evacuated and flushed with high-purity argon gas. Then 6 ml of alkaline $NaBH_4$ solution which contained 10 wt.% $NaBH_4$ and 10 wt.% NaOH was injected into the rubber plug sealed flask through a syringe. The volume of hydrogen generated from the hydrolysis reaction of $NaBH_4$ solution in the presence of CoO catalysts was measured using the water-displacement method. The reaction temperature was controlled by immersing the flask in a temperature-controlled water bath which was equipped with magnetic stirring apparatus. Hydrolysis experiments were also conducted using different quantities of CoO catalysts at various temperatures in the range of 10–50 °C.

3. Results and discussion

3.1. Synthesis and characterization of CoO nanocrystals

Fig. 1a shows the low-magnification TEM image of the as-prepared octahedral CoO nanocrystals with a typical size varying from 40 to 50 nm. These nanocrystals typically have a parallelogrammic shape which actually corresponds to the two-dimensional projection of octahedral nanocrystals with the base plane approximately

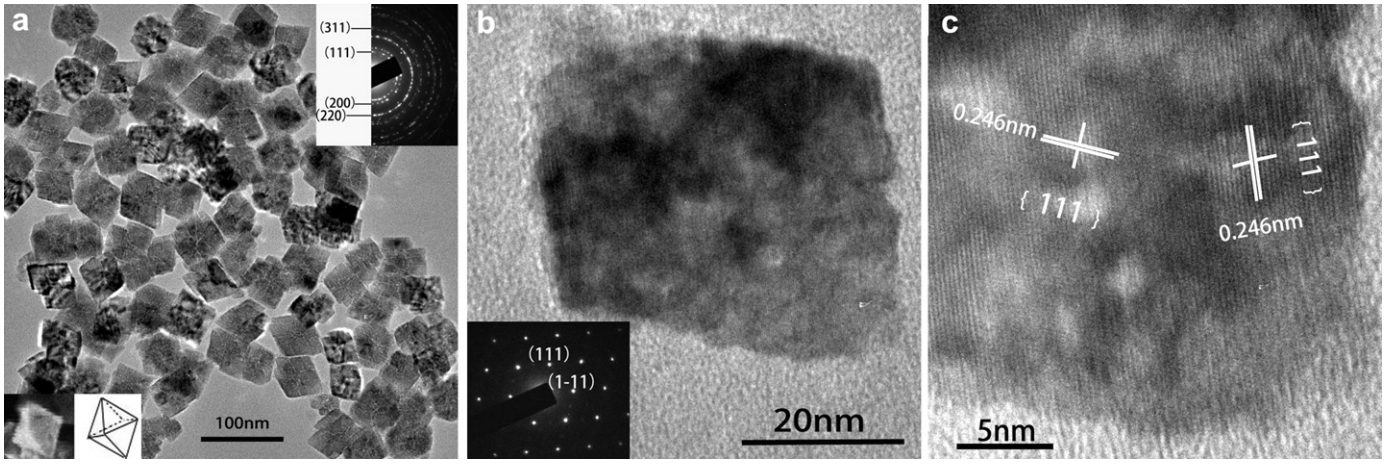

Fig. 1. (a) Low-magnification TEM image of octahedral CoO nanocrystals along with the SAED pattern (up inset). The insets below are the SEM image of a single nanocrystal and its schematic diagram showing the octahedral morphology. (b) High-magnification TEM image of a single octahedral CoO nanocrystal along with its SAED pattern (inset) viewed in the [−101] zone axis. (c) HRTEM image of a single octahedral nanocrystal showing the lattice fringes corresponding to cubic phase of CoO.

perpendicular to the supporting films. The octahedral shape is clearly revealed from the magnified SEM image (Fig. 1a inset below). An important aspect of these octahedral nanocrystals is that they are not perfect single crystals with smooth surfaces. Crack-like features or micro-grooves can be found in these nanocrystals, which may have great impact to the catalytic properties that will be discussed later. The selected area electron diffraction (SAED) pattern (Fig. 1a up inset) recorded from randomly distributed nanocrystals exhibits diffraction rings that correspond to face centered cubic (fcc) CoO. To further verify the structure of the nanocrystals, SAED pattern was recorded from isolated octahedral nanocrystals. Fig. 1b shows the high-magnification TEM image of a single octahedral nanocrystal along with its SAED pattern. Obviously the SAED pattern (Fig. 1b inset) reveals single crystalline characteristics and the {111} diffraction spots corresponding to the facets of octahedron are evident. High-resolution TEM (HRTEM) image (Fig. 1c) taken from the same nanocrystal also exhibits lattice fringes corresponding to the {111} planes of fcc CoO at the edge portion. Moreover, the angle between neighboring sides of projected parallelogram is about 60°. These results suggest that the octahedral nanocrystal is exposed with {111} facets.

Fig. 2a demonstrates the TEM image of CoO nanocrystals that have a near-spherical morphology. The particle size determined from TEM image is ranging from 8 to 13 nm. The recorded SAED pattern (Fig. 2a inset) exhibits diffraction rings that agree well with fcc CoO. The HRTEM image recorded from separate nanocrystals (Fig. 2b) exhibits lattice fringes that go straight throughout the whole nanocrystals, indicating single-crystalline characteristics. The measured lattice spacing of 0.246 nm in the image corresponds well to the {111} planes of fcc CoO.

The synthetic parameters have great influences to the size and phase of nanocrystals. The particle size and crystalline phase is sensitive to the quantity of added $Co(OAc)_2 \cdot 4H_2O$, TOP and reaction temperature. For example, octahedral CoO nanocrystals with a smaller size of 10–20 nm (see Fig. 3a) was obtained when the quantity of $Co(OAc)_2 \cdot 4H_2O$ was reduced to 0.25 mmol and that of TOP was increased to 3 mmol. The size-inhibiting effect of TOP is very evident when the reaction solution contains a high concentration of TOP. The reaction temperature does not have significant effect on the size of nanocrystals, however it greatly affects the crystalline phase. When the reaction temperature exceeded 250 °C, the reducing capacity of oleylamine was strong enough to transform Co(II) to Co(0) directly, resulting in Co nanospheres (see Fig. 3b) that have a multi-spike morphology and a size over 100 nm. The recorded SAED pattern (Fig. 3b inset) confirms that these nanospheres have a crystalline phase of fcc Co. These Co nanospheres were self-assembled into curves or close-packed

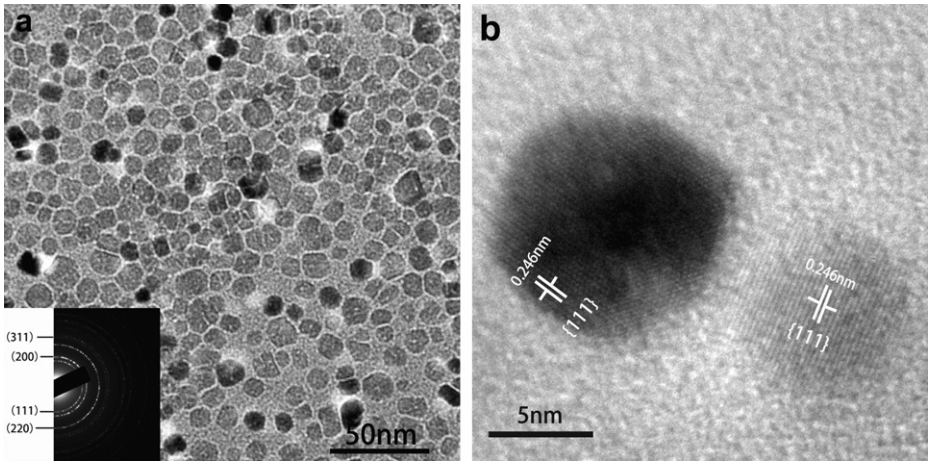

Fig. 2. Low-magnification TEM image (a) with a SAED pattern (insert) and HRTEM image (b) of near-spherical CoO nanocrystals.

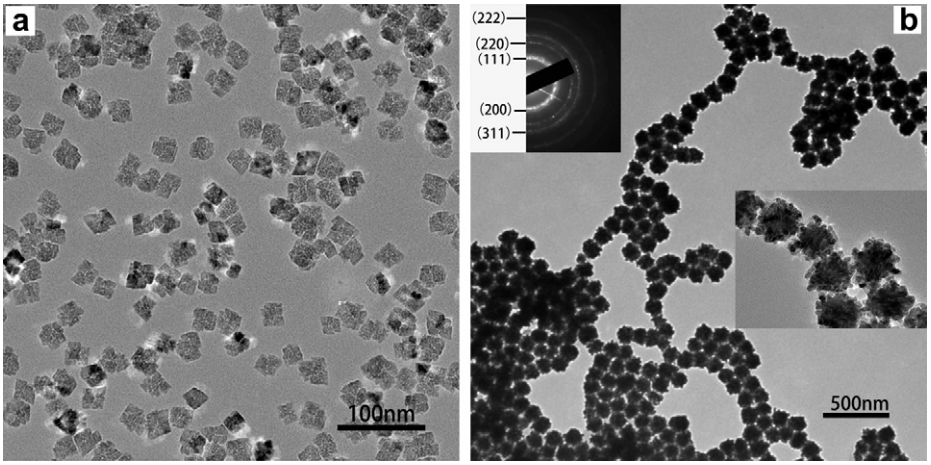

Fig. 3. (a) TEM image of octahedral CoO nanocrystals with a smaller size (~25 nm). (b) TEM image of Co nanospheres. The insets are the SAED pattern and magnified image, respectively.

arrays due to magnetic interactions. Similar phenomenon was noticed in self-assembled Ni–Co nanoparticle rings [23], and Co nanospheres with a size of ~500 nm [24]. If the reaction temperature was under 190 °C, $Co(OAc)_2 \cdot 4H_2O$ did not decompose, and the solution would maintain blue violet and transparent. The obtained Co nanospheres give us an opportunity to compare the catalytic performance between metallic Co and its oxide on $NaBH_4$ hydrolysis.

The XRD patterns of as-prepared CoO nanocrystals with different sizes and Co nanospheres are shown in Fig. 4. The diffraction peaks at 2θ values of 36.6°, 42.5°, 61.6° and 73.8° for the CoO samples can be assigned to the (111), (200), (220) and (311) planes of fcc CoO, respectively. There is no evidence for the existence of crystalline impurities based on XRD or SAED pattern though CoO nanocrystals are hard to be obtained in a pure form. Impurities such as Co and Co_3O_4 formed by intentional over-oxidation were often detected [25]. The XRD pattern shown in curve c agrees well with that of fcc Co.

To verify the chemical states of the as-prepared CoO nanocrystals, XPS spectra were recorded. Fig. 5 shows the XPS spectra of Co 2p and O 1s regions of the octahedral nanocrystals. The peaks at 780.0 eV and 795.2 eV are attributed to Co (II) $2p_{3/2}$ and Co (II) $2p_{1/2}$ energy levels, respectively, which is in agreement with the reported values for fcc CoO [26]. The O 1s peak at 529.1 eV (Fig. 5b) also suggests the oxide form of CoO. For the near-spherical CoO sample, similar spectra of Co 2p and O 1s were detected (data not shown here). These results suggest that the chemical states of the as-prepared octahedral and near-spherical nanocrystals should be in the form of CoO.

The growth mechanism of nanocrystals with different shapes is a complex issue. The resulted two types of morphologies of CoO are related to the controlling effects of surfactants on the growth rate of formed nuclei. For the formation of octahedral nanocrystals, cobalt acetate decomposed at a relatively low speed in oleylamine for the hindrance effect of TOP. The solution remained transparent at the reaction temperature of 240 °C for 20 min, after which dark brown precipitate was visible. The low decomposing speed allows CoO nanocrystals to grow at a thermodynamically balanced condition. Additionally, the interaction between oleylamine and {111} facets may be stronger than that on other facets. A calculation on different surfaces of cubic CoO indicates that the surface energy of (111) facets is higher than other low-index facets (e.g. (100) and (110) facets) [19]. Therefore the absorbed oleylamine molecules may protect {111} facets and eventually lead to the formation of octahedron nanocrystals with eight exposed {111} facets. During the synthesis of near-spherical nanocrystals, the solution color changed from transparent brown to non-transparent yellow very rapidly in 1 min after the solution temperature exceeded 250 °C, indicating a fast decomposition of cobalt complex which yielded a large number of crystal nuclei. Due to the absence of hindrance effect of TOP, the followed growth process would make these nuclei to grow roughly equally on each crystalline facet, resulting in a near-spherical morphology.

3.2. Catalytic properties

3.2.1. Hydrogen generation by using as-prepared nanocrystals

Alkaline $NaBH_4$ solution at a pH value of 14 can be kept stable at room temperature for 430 days [2]. Catalysts added would drastically shorten this stable period. To compare the catalytic behaviors of as-prepared octahedral CoO, near-spherical CoO and Co nanosphere samples, the initial concentration of $NaBH_4$ and NaOH in the solution was either 10% and the hydrolysis reaction temperature was maintained at 303 K. The plots of H_2 generation volume as a function of time of three as-prepared samples are shown in Fig. 6a. It can be seen that the total H_2 volume generated using

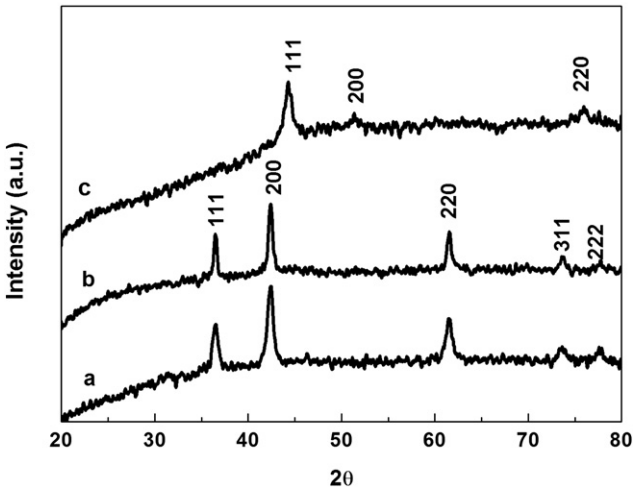

Fig. 4. XRD patterns of near-spherical (a) and octahedral (b) CoO nanocrystals, and Co nanospheres (c).

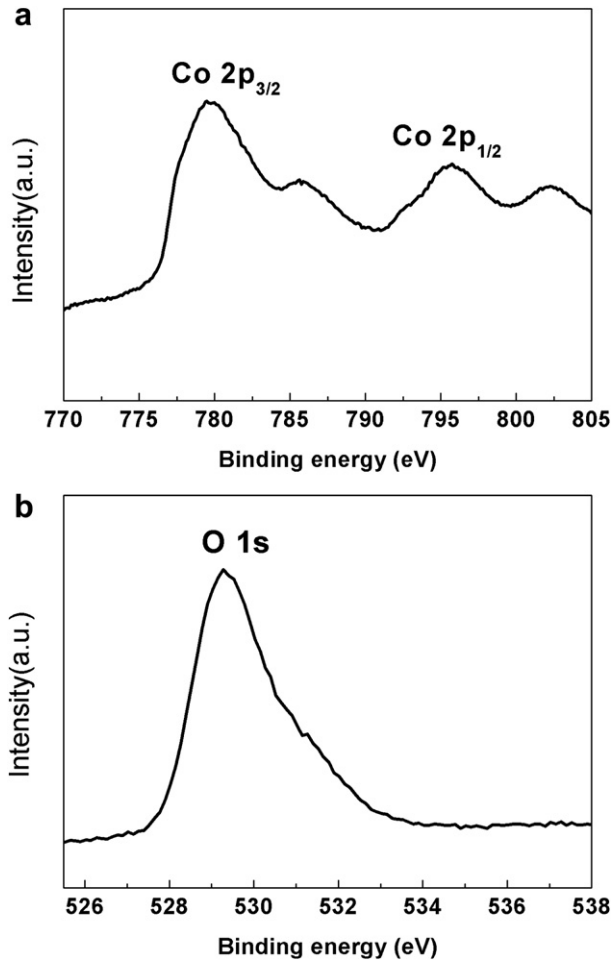

Fig. 5. XPS spectra of Co 2p (a) and O 1s (b) regions for octahedral CoO nanocrystals.

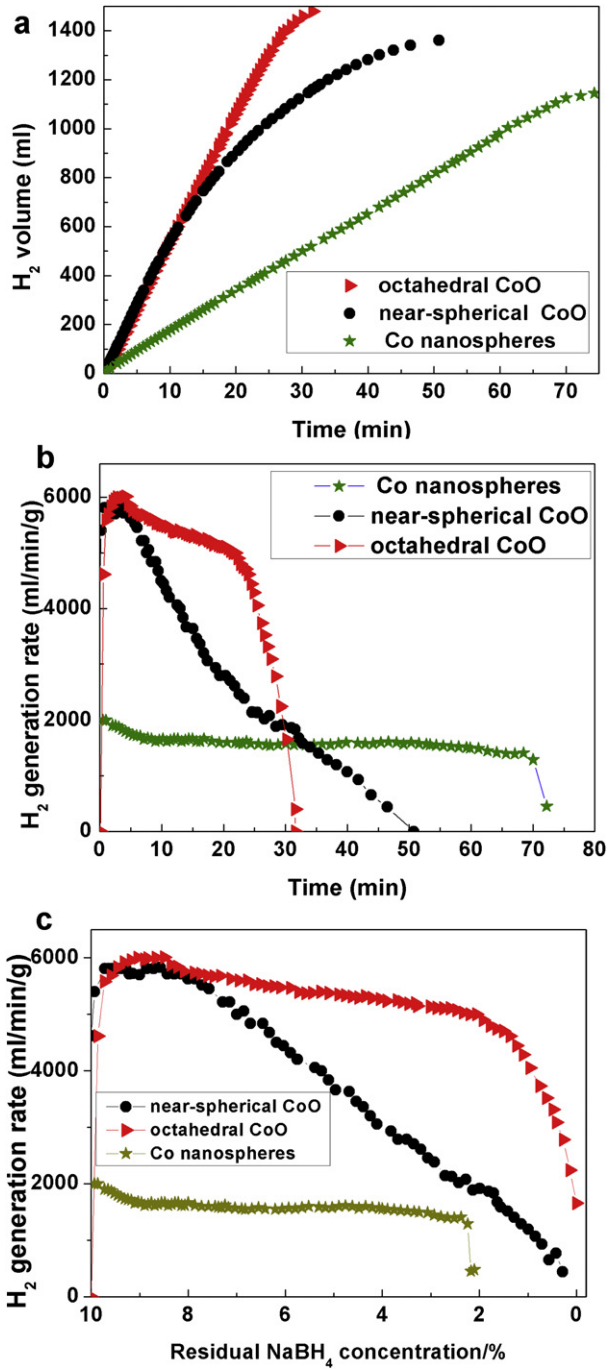

Fig. 6. The curves of hydrogen generation volume (a) and hydrogen generation rates (b) as a function of time for as-prepared octahedral CoO, near-spherical CoO and Co nanosphere catalysts at 303 K (the catalyst quantity is 10 mg for each run). (c) is the corresponding hydrogen generation rates as a function of residual $NaBH_4$ concentration in solutions at 303 K. The initial $NaBH_4$ concentration is 10 wt.%.

octahedral CoO is about 1500 ml, approximating the maximum volume that the added $NaBH_4$ can provide. However, for Co nanospheres, only 1145 ml of H_2 is produced, indicating a portion of loss of $NaBH_4$. The total H_2 volume generated using near-spherical CoO is also higher than that of Co nanospheres but slightly lower than that of octahedral CoO. Table 1 summarizes the maximum H_2 generation rates in borohydride solutions catalyzed by various catalysts reported in literature and CoO nanocrystals synthesized in this study. The maximum H_2 generation rate of the CoO nanocrystals synthesized in this study exceeds every transition metal catalyst and most noble metal contained catalysts performed at the same reaction temperature. Furthermore, when the quantity of octahedral CoO nanocrystals is increased to 20 mg with other conditions fixed, the maximum H_2 generation rate is up to 8333 ml min^{-1} g^{-1} at 303 K. These results indicate that CoO nanocrystals have a very high catalytic activity and can be an excellent substitution for noble metal catalysts in the catalytic generation of H_2 via hydrolysis of $NaBH_4$.

To investigate the stability of H_2 generation rate in the entire catalytic process, we plot the curve of H_2 generation rate vs time (Fig. 6b) which can be obtained from the differential curve of H_2 volume vs time shown in Fig. 6a. As shown in Fig. 6b, the Co nanospheres display the lowest but the most stable H_2 generation rate (about 1650 ml min^{-1} g^{-1} at 303 K), which is in accordance with the reported result that pure Co showed low catalytic activity except for the case that it combined with other elements such as B and P [27]. The near-spherical CoO nanocrystals display rather high catalytic activity (H_2 generation rate is about 5825 ml min^{-1} g^{-1}) only at the initial stage, after that it gains a continuous and rapid drop. In contrast, the octahedral CoO nanocrystals show an extraordinary high and relatively steady activity toward $NaBH_4$ hydrolysis, though the H_2 generation rate decreases slowly from 5998 to 5165 ml min^{-1} g^{-1} in the middle process, and finally gains a sharp decay due to reaction cessation. This result demonstrates that octahedral CoO nanocrystals have more stable catalytic activity than near-spherical CoO nanocrystals.

Table 1
Comparison of the maximum H_2 generation rates obtained by using various catalysts.

Catalyst type	Catalyst weight (mg)	Hydrides	Maximum H_2 generation rate (ml min^{-1} g^{-1})	Reference
Pt/C	100	$NaBH_4$	23,000 (298 K)	[3]
Co@Pt core–shell	7	NH_3BH_3	5869 (303 K)	[8]
Cu/Co_3O_4	12	NH_3BH_3	1411 (298 K)	[11]
Co–P–B	15	$NaBH_4$	2120 (298 K)	[13]
Co–Ni–P–B	15	$NaBH_4$	2400 (298 K)	[27]
$Pt/LiCoO_2$	20	$NaBH_4$	3680 (303 K)	[28]
Raney Co	500	$NaBH_4$	267.5 (293 K)	[34]
Raney $Ni_{50}Co_{50}$	500	$NaBH_4$	648.2 (293 K)	[34]
Pt/CoO	3.8	$NaBH_4$	350 (293 K)	[35]
Octahedral CoO	10	$NaBH_4$	2400 (293 K)	This study
Octahedral CoO	10	$NaBH_4$	5950 (303 K)	This study
Octahedral CoO	20	$NaBH_4$	8333 (303 K)	This study
Octahedral CoO	10	$NaBH_4$	3888 (calculated) (298 K)	This study
Near-spherical CoO	10	$NaBH_4$	5890 (303 K)	This study

Fig. 6c shows the curve of H_2 generation rate vs residual $NaBH_4$ concentration. As the reaction proceeds, the $NaBH_4$ concentration decays (the initial concentrations of $NaBH_4$ and NaOH are all 10 wt.%), and the H_2 generation rate varies for different catalysts. The near-spherical CoO nanocrystals are most sensitive to the actual $NaBH_4$ concentration, and corresponding H_2 generation rate begins to drop rapidly when the residual $NaBH_4$ concentration is less about 8 wt.%. In contrast, the octahedral CoO exhibits a rather stable H_2 generation rate until the residual $NaBH_4$ concentration is less than 2 wt.%. The Co nanospheres also display a very stable H_2 generation rate, but unfortunately its value is much lower than that of CoO counterpart.

We also found that the gradually declining catalytic behavior of CoO nanocrystals in alkaline $NaBH_4$ solution (see Fig. 6b) differed from that of Co_3O_4-supported catalyst which sometimes demonstrated characteristics of second-order reaction distinguished by two peaks in the curve of H_2 generation rate vs time [12]. The activation time before the coming of the highest catalyst rate for Co_3O_4 was near 5 min in $NaBH_4$ alkaline solution [28] and 52 min in $HN_3 \cdot BH_3$ solution [11]. In contrast, the activation time for CoO nanocrystals examined in this study was less than 100 s. The short activation time in the catalytic process is also an advantage for practical applications.

3.2.2. *Effects of initial $NaBH_4$ concentration to the catalytic performances*

Considering that the catalytic performances of as-prepared nanocrystals depend closely with actual $NaBH_4$ concentration, we also investigated the effects of initial $NaBH_4$ concentrations at 5 wt.% and 2.5 wt.%, respectively. Since CoO nanocrystals exhibit much better catalytic activities than Co nanospheres, we only focused our study on CoO nanocrystal samples.

Fig. 7 shows the curves of hydrogen generation volume and hydrogen generation rates as a function of time for octahedral CoO nanocrystals at initial $NaBH_4$ concentrations of 5 wt.% and 2.5 wt.%, respectively. The NaOH concentration, catalyst quantity and temperature are kept at 10 wt.%, 10 mg and 303 K, respectively. The obtained maximum H_2 generation rates are 6154 and 5890 ml min^{-1} g^{-1} for initial $NaBH_4$ concentration at 5 wt.% and 2.5 wt.%, respectively. These values are very close to that in the case of initial $NaBH_4$ concentration of 10 wt.%, which indicates that the maximum H_2 generation rate of octahedral CoO nanocrystals is not sensitive to the decrease of initial $NaBH_4$ concentration. It also can be seen in Fig. 7b that the H_2 generation rates begin to drop

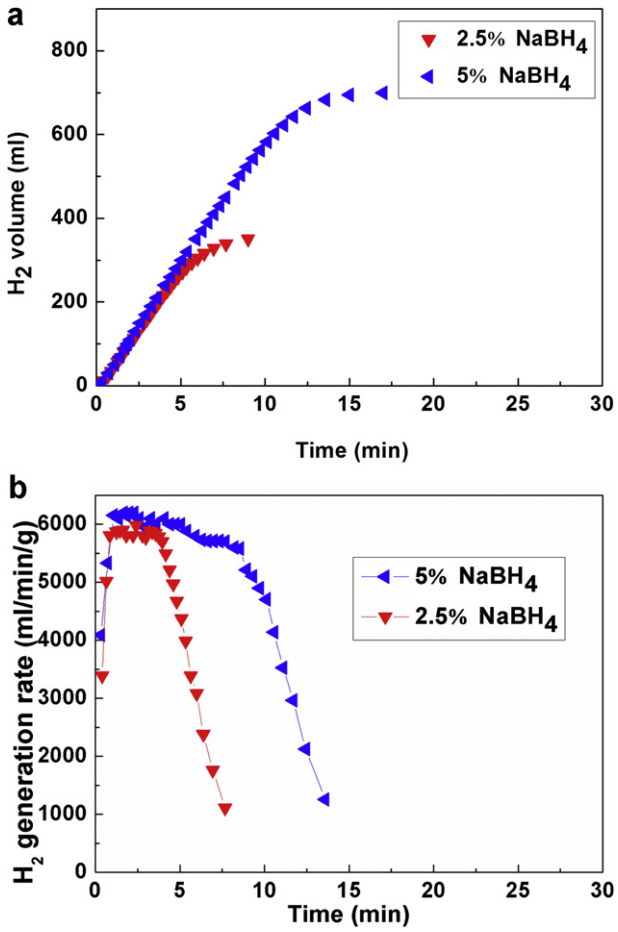

Fig. 7. The curves of hydrogen generation volume (a) and hydrogen generation rate (b) as a function of time for octahedral CoO nanocrystals in solutions at 303 K with initial $NaBH_4$ concentration of 5 wt.% and 2.5 wt.%, respectively (the catalyst quantity is 10 mg for each run and NaOH concentration is 10 wt.%).

significantly only at the late stage, although the sample tested at 2.5 wt.% of initial $NaBH_4$ concentration tends to drop earlier than that at 5 wt.%. For near-spherical CoO nanocrystals, the obtained maximum H_2 generation rates are 5005 and 3713 ml min^{-1} g^{-1} for initial $NaBH_4$ concentration at 5 wt.% and 2.5 wt.%, respectively (Fig. 8). Compared to the case of 10 wt.% of initial $NaBH_4$ concentration (see Table 1), the maximum H_2 generation rate decreases significantly, especially in the case of low initial $NaBH_4$ concentration. This reflects the sensitivity of near-spherical CoO nanocrystals to the drop of initial $NaBH_4$ concentration. In addition, drastic decline of H_2 generation rate occurs at the early stage for near-spherical CoO nanocrystals, which is quite different from that of octahedral CoO nanocrystals. This result demonstrates that the octahedral CoO nanocrystals have much better catalytic stability than that of near-spherical CoO counterpart.

With regard to the effect of $NaBH_4$ concentration on the hydrogen generation rate, various results have been reported in literature. For example, the hydrogen generation rate decreased with increasing $NaBH_4$ concentration in the case of amorphous Co–B [14], Ru [6] and supported Co [29] catalysts. The reason was explained to be the increasing solution viscosity. Similar to the case of octahedral CoO nanocrystals, some researchers reported that the hydrolysis rate was irrelevant to $NaBH_4$ concentration [30–32], whereas some other researchers demonstrated positive-order kinetics that hydrogen generation rate increased with $NaBH_4$ concentration [4,33], which is similar to the case of near-spherical

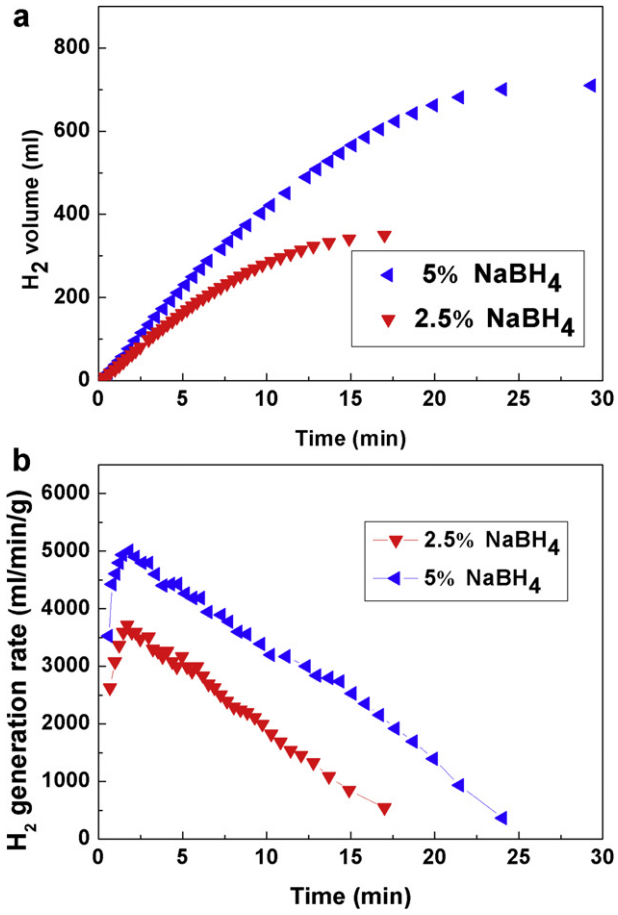

Fig. 8. The curves of hydrogen generation volume (a) and hydrogen generation rate (b) as a function of time for near-spherical CoO nanocrystals in solutions at 303 K with initial $NaBH_4$ concentration of 5 wt.% and 2.5 wt.%, respectively (the catalyst quantity is 10 mg for each run and NaOH concentration is 10 wt.%).

CoO nanocrystals. However, hardly any attention has been paid to the grain shape effect of catalysts that have same chemical compositions, which is not only important in the $NaBH_4$ hydrolysis but also in other catalytic applications. Our results show that although near-spherical CoO nanocrystals have smaller dimensions, their catalytic activities are more dependent on $NaBH_4$ concentration and less superior to octahedral CoO counterpart.

3.2.3. *Effects of temperature on the catalytic performances*

The effects of solution temperature on catalytic performances of CoO nanocrystals are demonstrated in Fig. 9a and Fig. 9b. As expected, the H_2 generation rate increases with the temperature. The values of rate constant k at different temperatures are calculated from the slope of the initial linear part of each plot. The k values of octahedral and near-spherical CoO nanocrystals at different temperatures are approximately equal. From the slope of Arrhenius plot shown in Fig. 9c, the Arrhenius activation energies of octahedral and near-spherical CoO nanocrystals are calculated to be about 58.5 and 59.7 kJ mol^{-1}, respectively. These Arrhenius activation energies are comparable to the reported value of 56 kJ mol^{-1} of Ru catalyst supported on IRA400 [6], and lower than that (68.87 kJ mol^{-1}) of anisotropy Co–B catalyst [14].

It also can be noted that the H_2 generation rate of near-spherical CoO nanocrystals is almost the same as octahedral counterpart at higher temperatures (313 and 323 K). When the temperature is below 313 K, the H_2 generation rate for near-spherical nanocrystals drops more rapidly than the octahedral one does. The reason may

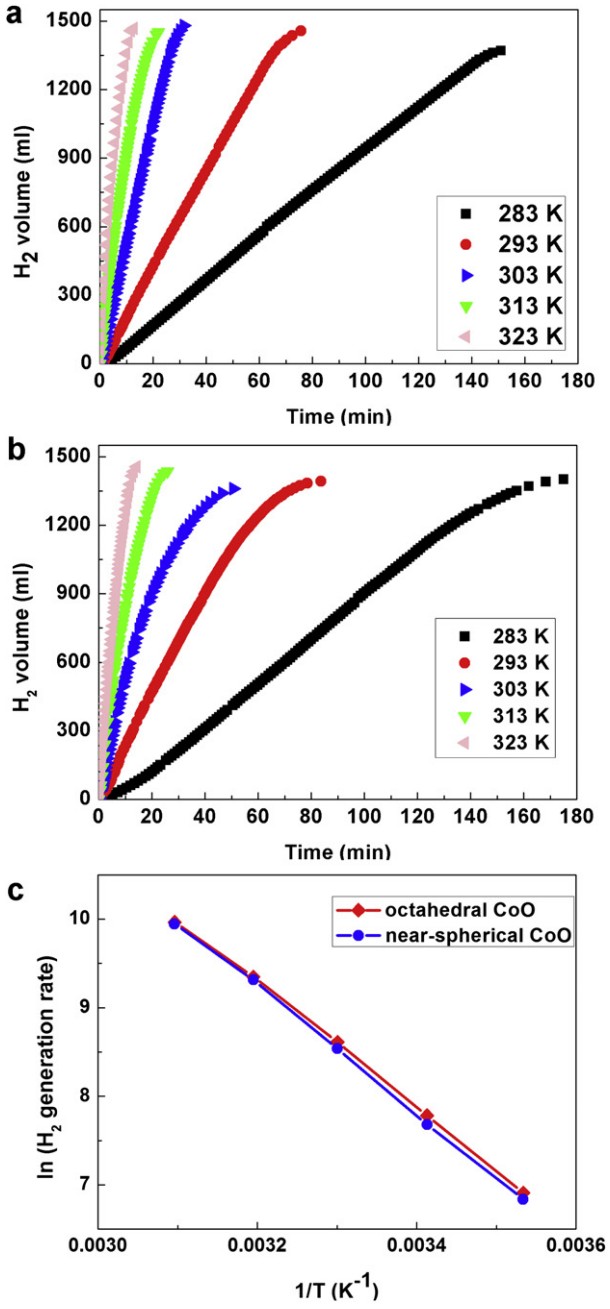

Fig. 9. The hydrogen generation rates for octahedral (a) and near-spherical (b) CoO nanocrystals at different temperatures in solutions containing 10 wt.% NaOH, 10 wt.% $NaBH_4$ and 10 mg catalyst. (c) The corresponding Arrhenius plots obtained from data shown in (a) and (b).

be due to the reduced molecular motions at lower temperature. As the reaction goes on, $NaBH_4$ concentration is decreased and it is relatively difficult for near-spherical CoO nanocrystals with smooth surface to capture more $NaBH_4$. Therefore the drop of catalytic activity is unavoidable. However for octahedral CoO nanocrystals with exposed high-energy {111} facets [19] plus unsmoothed surfaces, it appears to be easier to seize $NaBH_4$ so that the decreasing $NaBH_4$ concentration is not very influential. At higher temperature, the molecular motion is accelerated and the occasions for catalyst to meet $NaBH_4$ increase too. Therefore the ability for catalysts to seize $NaBH_4$ is less important. In brief, the surface condition and exposed crystal facet of catalyst play an important role in its catalytic behavior.

4. Conclusions

CoO nanocrystals with octahedral and near-spherical shapes have been synthesized in a facile chemical solution method, and they have been found to be highly active for the H_2 generation from the catalytic hydrolysis of alkaline $NaBH_4$ solutions. The maximum H_2 generation rate of the as-prepared CoO nanocrystals exceeds most reported values of transition metal or noble metal contained catalysts performed on similar conditions. For octahedral CoO nanocrystals, a maximum H_2 generation rate of 8333 ml min^{-1} g^{-1} has been obtained at 303 K. The crystal shape of as-prepared CoO nanocrystals also affects their catalytic activity and stability. Compared to the near-spherical counterpart, the H_2 generation rate of octahedral CoO nanocrystals appear not to be sensitive to the decrease of $NaBH_4$ concentration and are more stable in solution. The Arrhenius activation energies of octahedral and near-spherical CoO nanocrystals are determined to be about 58.5 and 59.7 kJ mol^{-1}, respectively. The results obtained in this study demonstrate that CoO nanocrystals can be a low-cost and high-efficiency catalyst for the substitution of noble metal catalysts in the H_2 generation from the hydrolysis of borohydrides.

Acknowledgments

The authors gratefully acknowledge financial support from the National Outstanding Youth Science Foundation of China (Grant no. 50825101), and Fundamental Research Funds for the Central Universities of China (Grant no. 2011121003).

References

[1] T.J. Clark, G.R. Whittell, I. Manners, Inorg. Chem. 46 (2007) 7522.
[2] H.I. Schlesinger, H.C. Brown, A.E. Finholt, J.R. Gilbreath, H.R. Hoekstra, E.K. Hyde, J. Am. Chem. Soc. 75 (1953) 215.
[3] Y. Bai, C. Wu, F. Wu, B. Yi, Mater. Lett. 60 (2006) 2236.
[4] G. Guella, C. Zanchetta, B. Patton, A. Miotello, J. Phys. Chem. B 110 (2006) 17024.
[5] P. Krishnan, T.H. Yang, W.Y. Lee, C.S. Kim, J. Power Sources 143 (2005) 17.
[6] S.C. Amendola, S.L. Sharp-Goldman, M.S. Janjua, N.C. Spencer, M.T. Kelly, P.J. Petillo, M. Binder, Int. J. Hydrogen Energy 25 (2000) 969.
[7] H. Guo, Y. Chen, X. Chen, R. Wen, G.H. Yue, D.L. Peng, Nanotechnology 22 (2011) 195604.
[8] J.M. Yan, X.B. Zhang, T. Akita, M. Haruta, Q. Xu, J. Am. Chem. Soc. 132 (2010) 5326.
[9] X. Yang, F. Chen, Z. Tao, J. Chen, J. Power Sources 196 (2011) 2785.
[10] V.I. Simagina, O.V. Komova, A.M. Ozerova, O.V. Netskina, G.V. Odegovaa, D.G. Kellerman, O.A. Bulavchenko, A.V. Ishchenko, Appl. Catal. A Gen. 394 (2011) 86.
[11] Y. Yamada, K. Yano, Q. Xu, S. Fukuzumi, J. Phys. Chem. C 114 (2010) 16456.
[12] P. Krishnan, K.L. Hsueh, S.D. Yim, Appl. Catal. B Environ. 77 (2007) 206.
[13] N. Patel, R. Fernandes, A. Miotello, J. Power Sources 188 (2009) 411.
[14] S.U. Jeong, R.K. Kima, E.A. Chob, H.J. Kimb, S.W. Namb, I.H. Ohb, S.A. Hong, S.H. Kim, J. Power Sources 144 (2005) 129.
[15] B.H. Liu, Q. Li, Int. J. Hydrogen Energy 33 (2008) 7385.
[16] K.M. Nam, J.H. Shim, D.W. Han, H.S. Kwon, Y.M. Kang, Y. Li, H. Song, W.S. Seo, J.T. Park, Chem. Mater. 22 (2010) 4446.
[17] V.R. Choudhary, R. Jhaa, P. Janaa, Catal. Commun. 10 (2008) 205.
[18] H. Yang, J. Ouyang, A. Tang, J. Phys. Chem. B 111 (2007) 8066.
[19] D.S. Wang, X.L. Ma, Y.G. Wang, L. Wang, Z.Y. Wang, W. Zheng, X.M. He, J. Li, Q. Peng, Y. Li, Nano Res. 3 (2010) 1.
[20] R. Bartsch, C. Tanielian, J. Catal. 35 (1974) 353.
[21] Y. Teng, H. Sakurai, A. Ueda, T. Kobayashi, Int. J. Hydrogen Energy 24 (1999) 355.
[22] Y. Zhang, J. Zhu, X. Song, X. Zhong, J. Phys. Chem. C 112 (2008) 5233.
[23] M.J. Hu, Yang Lu, S. Zhang, S.R. Guo, B. Lin, M. Zhang, S.H. Yu, J. Am. Chem. Soc. 130 (2008) 11606.
[24] C.W. Kim, H.G. Cha, Y.H. Kim, A.P. Jadhav, E.S. Ji, D.I. Kang, Y.S. Kang, J. Phys. Chem. C 113 (2009) 5081.
[25] N.R. Jana, Y. Chen, X. Peng, Chem. Mater. 16 (2004) 3931.
[26] C.R. Brundle, T.J. Chung, D.,W. Rice, Surf. Sci. 60 (1976) 286.
[27] R. Fernandees, N. Patel, A. Miotello, J. Hydrogen Energy 34 (2009) 2893.
[28] Z. Liu, B. Guo, S.H. Chan, E.H. Tang, L. Hong, J. Power Sources 176 (2008) 306.
[29] W. Ye, H. Zhang, D. Xu, L. Ma, B. Yi, J. Power Sources 164 (2007) 544.
[30] Y. Kojima, K.I. Suzuki, Y. Kawai, J. Power Sources 155 (2006) 325.
[31] J.S. Zhang, W.N. Delgass, T.S. Fisher, J.P. Gore, J. Power Sources 164 (2007) 772.
[32] S.C. Amendola, S.L. Sharp-Goldman, M.S. Janjua, M.T. Kelly, P.J. Petillo, M. Binder, J. Power Sources 85 (2000) 186.
[33] R. Pena-Alonso, A. Sicurelli, E. Callone, G. Carturan, R. Raj, J. Power Sources 165 (2007) 315.
[34] B.H. Liu, Z.P. Li, S. Suda, J. Alloys Compd. 415 (2006) 288.
[35] Y. Kojima, K. Suzuki, K. Fukumoto, M. Sasaki, T. Yamamoto, Y. Kawai, H. Hayashi, Int. J. Hydrogen Energy 27 (2002) 1029.